The Production of Neutrons by μ-Meson Capture in Lead, Magnesium, and Calcium*,†

ANNA MARIA CONFORTO‡ AND R. D. SARD§
Washington University, St. Louis, Missouri
(Received September 24, 1951)

Measurements are reported of the yield of disintegration neutrons from the capture of stopped negative μ-mesons in Pb, Ca, and Mg. A magnetized iron lens is used to separate μ-meson capture from other processes giving rise to neutrons associated with telescope anticoincidences. The functioning of the lens is tested experimentally by observation of decay electrons from stopped mesons; as a byproduct, the competition between capture ($\tau_-=1$ μsec for Mg) and natural decay ($\tau_0=2.15$ μsec) is confirmed. The telescope coincidence and anticoincidence rates are in excellent agreement with recent absolute determinations of the μ-meson spectrum at sea level.

With Pb, there is a striking increase in the coherent neutron rate in switching from focusing positive to focusing negative mesons. This confirms the interpretation of earlier experiments without magnetic field as demonstrating neutron emission resulting from μ-meson capture. The average number of disintegration neutrons per capture appears to be 1.47 ± 0.13 (statistical standard error), as compared with the value 2.16 ± 0.15 (statistical standard error) obtained by Crouch and Sard in an underground experiment. Systematic errors can account for the discrepancy; it is felt that somewhat more weight should be attached to the latter figure. With both Mg and Ca, there is little, if any, neutron production in μ-meson capture. The neutron detecting efficiency is the same as for Pb, but the ratio of neutrons detected to mesons captured is (0.6 ± 0.5) percent for Mg and for Ca, in contrast with (3.1 ± 0.3) percent for Pb. Despite the poor statistics of these preliminary measurements, it is clear that the average neutron multiplicity from Mg and Ca is considerably smaller than from Pb.

1. INTRODUCTION

IN order to study the μ-meson-nucleon interaction, we have begun a series of measurements of the neutron emission resulting from the capture of negative μ-mesons stopped in various elements. In the case of Pb, it has been shown[1,2] that μ-meson capture leads to the emission of neutrons in the range of energies up to about 10 Mev; these neutrons are presumably boiled out of the Tl nucleus as a result of the excitation provided by the neutron recoil in such a reaction as $P+\mu^-\rightarrow N+\nu$. No data for other stopping materials have as yet been published. The present paper reports measurements on Pb, Mg, and Ca. Lead was studied first, in order to confirm the interpretation of the earlier experiments and in order to check our technique. Measurements were then made with Mg and with Ca. The first results with these light absorbers indicated a surprisingly low yield of neutrons in the energy range of our detector, and it was decided to interrupt the measurements in order to improve the detecting efficiency of the system when working with absorbers of low density. As circumstances have since compelled us to suspend work on the experiment, we consider it worthwhile to report at this time the preliminary results obtained before the shut-down.

The earlier work[1,3] had shown that μ-meson capture is only one of various processes by which charged cosmic-ray particles produce disintegration neutrons, and it was necessary to design an experimental arrangement that would permit a clear separation of the neutron production by μ-meson capture. The magnetized-iron lens[4] is ideally suited for this purpose. It gives practically perfect focusing of μ-mesons in a certain momentum band, in our case 490–590 Mev/c on incidence and 0–219 Mev/c on emergence; thus an absorber placed beneath it, of not too great thickness, does not stop any telescope mesons of the wrong polarity. When the sense of the field is such as to focus positive mesons, there is, therefore, no contribution to the neutron coincidence rate from stopped negative mesons. Protons are not focused, because their ranges for the momenta required are too short, even considering only ionization loss. Electrons are not focused because of Coulomb scattering and radiation loss in the iron (30.5 cm Fe is about 17 radiation lengths). π-mesons are scarce at sea level; any that arrived in the telescope would have their focusing spoiled if nuclear energy loss or scattering occurred. In fact, it is likely[5–7] that the cross section for such an interaction is close to the geometrical area of the Fe nucleus; with 30.5 cm Fe there is then only a 10 percent chance of a π-meson getting through the lens without a nuclear collision. Since stopped positive

* The results given here were presented at the New York Meeting of the American Physical Society, February 3, 1951 [Phys. Rev. **82**, 335 (1951)]. The present article, except for the results on Mg and Ca, is a condensation of a thesis presented by Anna Maria Conforto to the Board of Graduate Studies of Washington University in October, 1950 in partial fulfillment of the requirements for the degree of Doctor of Philosophy.

† Supported by the joint program of the ONR and AEC.

‡ Now at the University of Rome, Rome, Italy.
§ Now on leave, as Fulbright Fellow at the University, Manchester, England.

[1] Sard, Ittner, Conforto, and Crouch, Phys. Rev. **74**, 97 (1948).
[2] G. Groetzinger and G. W. McClure, Phys. Rev. **74**, 341 (1948); G. W. McClure and G. Groetzinger, Phys. Rev. **75**, 340 (1949).
[3] Sard, Conforto, and Crouch, Phys. Rev. **76**, 1134 (1949); Sard, Crouch, Jones, Conforto, and Stearns, Nuovo cimento **8**, 326 (1951); Fowler, Sard, Fowler, and Street, Phys. Rev. **78**, 323 (1950).
[4] Bernardini, Conversi, Pancini, Scrocco, and Wick, Phys. Rev. **68**, 109 (1945).
[5] Camerini, Fowler, Lock, and Muirhead, Phil. Mag. **41**, 413 (1950).
[6] K. H. Barker and C. C. Butler, Proc. Phys. Soc. (London) **A64**, 4 (1951).
[7] Bernardini, Booth, Lederman, and Tinlot, Phys. Rev. **82**, 105 (1951); Camac, Corson, Littauer, Shapiro, Silverman, Wilson, and Woodward, Phys. Rev. **82**, 325 (1951).

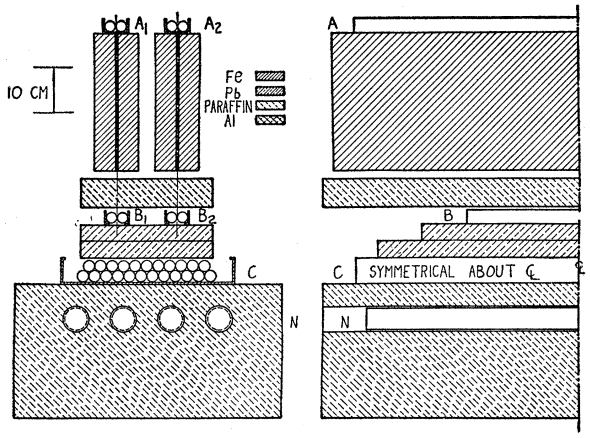

FIG. 1. The geometry of the experiment.

μ-mesons do not interact with nuclei, and since, as just explained, the contribution to the neutron coincidence rate from processes other than μ-meson capture is indifferent to the sense of the magnetic field,[8] the increase in the neutron coincidence rate when the current is reversed so as to focus negative rather than positive mesons must be ascribed exclusively to stopped negative μ-mesons.

2. EXPERIMENTAL APPARATUS

The apparatus was operated at St. Louis (160 meters, or 21 g cm^{-2} air, above sea level) under a thin roof of slate (2.7 g cm^{-2}) and wood (1.4 g cm^{-2}), equivalent to 4.0 g cm^{-2} air. Figure 1 shows the experimental layout. In order to double the counting rates, two lenses are used, mounted side by side; each lens has its own two-fold coincidence telescope, A_1B_1 and A_2B_2, respectively. The prompt coincidences (A_1B_1) and (A_2B_2) are mixed to give one output, designated as (AB). In this way, spurious coincidences due to wrong-sign particles zig-zagging through A_1 and B_2 or through A_2 and B_1 are eliminated. The iron bars constituting the lenses are 239 g cm^{-2} in vertical thickness, sufficient to eliminate completely the atmospheric soft component. Between them and the G-M tubes B is a slab of paraffin 6.3 cm thick. The main function of this barrier is to stop mesons that have just enough energy to get through the iron; these are subject to strong Coulomb scattering in the iron, and could mar the sign discrimination. The barrier also reduces the vulnerability of the telescope to side showers, reduces the efficiency of the neutron detecting system for neutrons from the iron, and increases, by its reflecting action, its efficiency for neutrons originating in the absorber. The absorber, 7.6 cm Pb in the drawing, is placed immediately beneath the B counters. Directly under the absorber is the C tray, containing 23 G-M tubes whose pulse outputs are connected in parallel. This tray fully covers the solid angle of the telescopes with the magnetic field on. The circuit records threefold prompt coincidences, ($AB:C_p$), as well as delayed coincidences ($AB:C_d$) from decay electrons resulting from stopped (AB) mesons. The rate at which stoppings occur in the absorber is clearly given by $(AB)-(AB:C_{pr})$, except for the background due to inefficiency and to stoppings in the counter walls (each 0.41-mm brass) and in the angle-iron supports for the absorber (1.24 g cm^{-2} when averaged over the 30.5×91.5 cm^2 absorber area). This background can be corrected for to a good approximation by subtracting off the value of $(AB)-(AB:C_{pr})$ in the absence of absorber. The block of paraffin under the C tray contains four thermal neutron counters,[9] N. The paraffin serves to thermalize the neutrons incident from above, some of which are then captured by the B^{10} nuclei in the counters to produce pulses, (N). Coincidences are recorded between these pulses (N) and events (AB), ($AB:N$); and between the pulses (N) and events ($AB:C_p$), ($ABC:N$).[10] Again, the difference $(AB:N)-(ABC:N)$ gives the rate of neutron production by stopped particles, while ($ABC:N$) gives the neutron production in penetrating events. The long mean life of a neutron in the detecting system requires the use of long coincidence gate pulses triggered by (AB) and ($AB:C_p$), while the lapse of time ($\sim$5 μsec) between emission of a neutron and its reaching thermal speed permits the starting of the gates to be delayed so as to avoid spurious coincidences due to prompt showers.

The circuits, shown in block diagram in Fig. 2, represent a combination of those developed by Sands[11] for recording the distribution in time of decay electrons from stopped mesons and those developed by Crouch[1,12] for recording neutron coincidences in delayed long gates. For obtaining the ($AB-C:N$) rate from the difference of ($AB:N$) and ($ABC:N$), it is essential that identical gate intervals be involved. Crouch's "master-slave" arrangement of gate generating circuits uses the end of the ($AB:N$) gate to terminate the ($ABC:N$) gate. The ($ABC:N$) gate also starts a little earlier, so that it extends beyond the ($AB:N$) gate at both ends. If this were not the case, some true ($ABC:N$) events would count as ($AB-C:N$) by occurring when the ($ABC:N$) gate is off but the ($AB:N$) gate on. On the other hand, use of the "operation recorder" chart has made it possible to recognize and reject cases in which the (N) pulse occurs outside the overlap period, as then there is an ($ABC:N$) pip on the chart without an ($AB:N$) pip.

The data reported in this paper were obtained in two periods in 1950, July 4–31, and August 31–October 3.

[8] The observed independence of the sense of the field for the ($ABC:N$) rate (see Tables I and II) supports this assumption.

[9] Proportional counters 5.1 cm×96.6 cm filled with $B^{10}F_3$ to 45 cm Hg pressure. The enriched BF_3 was obtained from the Isotopes Division, Atomic Energy Commission, Oak Ridge, Tennessee. The counters were made and filled by the N. Wood Counter Laboratory, 5646 Harper Avenue, Chicago, Illinois.

[10] Initially provision was also made for recording coincidences between neutron counts (N) and delayed coincidences ($AB:C_d$). As expected, none were observed (see Table I). When the circuit was modified for the second period of data taking, the ($ABC_d:N$) circuit was eliminated.

[11] Rossi, Sands, and Sard, Phys. Rev. **72**, 120 (1947).

[12] M. F. Crouch, thesis, Washington University, September, 1950.

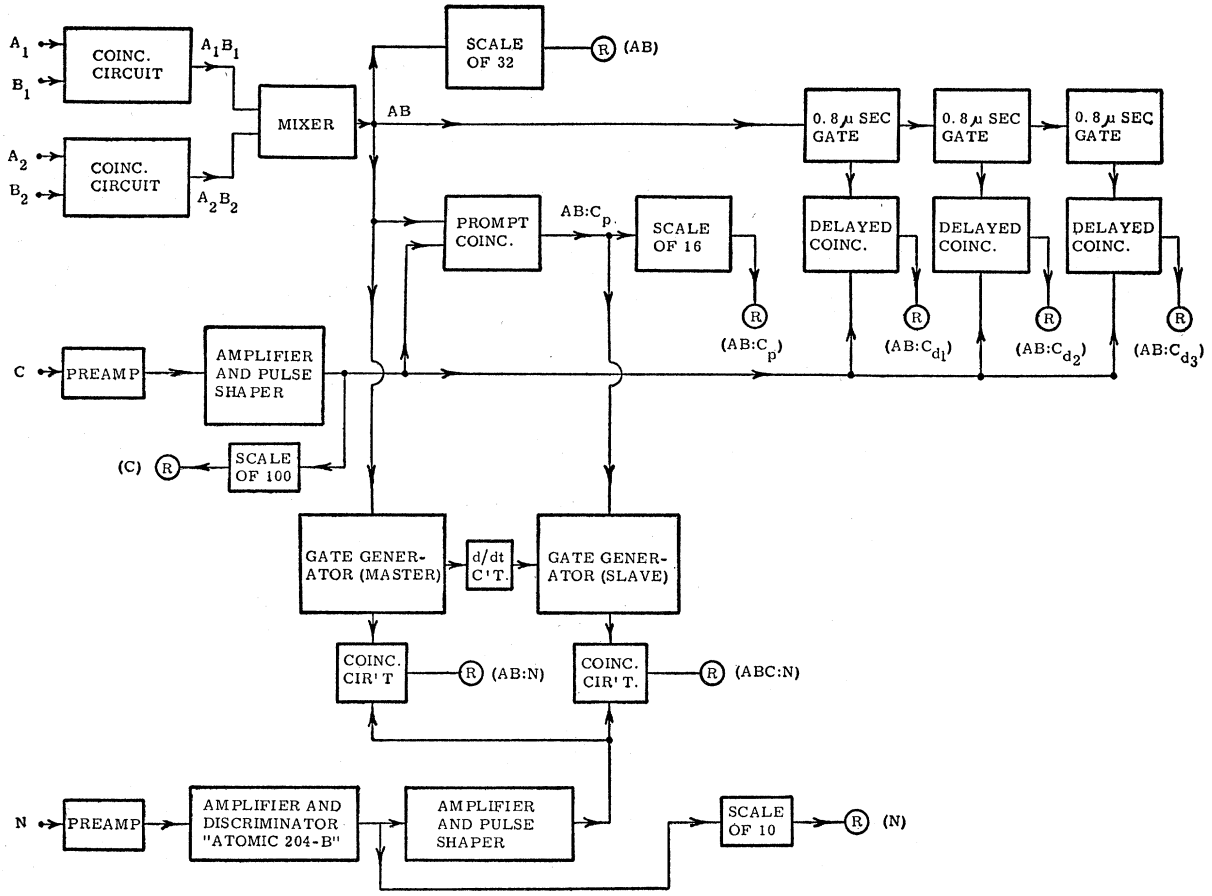

FIG. 2. Block diagram of the circuits. The symbol R stands for a "message register" (electromechanical counter) and its associated driving circuit and operation-recorder pen.

The description of the circuit given above refers to the second period of data taking (second Pb series, Mg, Ca) In the earlier period (first Pb series), the delayed coincidence circuit had only two channels, extending from 1.0 to 4.6 μsec and 4.5 to 8.0 μsec, respectively; the $(AB{:}N)$ and $(ABC{:}N)$ gates were each set independently at 188 μsec, with no "master-slave" circuit; and the C tray pre-amplifier did not have as high gain. In addition as has been already remarked,[10] a circuit for detecting events in which neutrons are associated with delayed coincidences, $(ABC_d{:}N)$ was used.

Each magnetic lens consists of two "Armco" iron bars wound with a single layer of enamelled copper wire. The coils (800 turns per bar) are connected in series so as to produce a large flux of induction around the closed iron "circuit." At the operating current of 7.0 amp, the field in the bars measures 15.0×10^3 gauss.

3. THE MEASURED COUNTING RATES

The rates measured in the first and second run are presented in Tables I and II, respectively. The tabulated rates are corrected for accidental coincidences, calculated from measured rates and resolving times. For $(AB{:}C_p)$ an additional correction—for decay electrons appearing in the prompt channel—has been made where necessary. The indicated uncertainties are simply the square root of the uncorrected number of counts divided by the duration. For the events of the first five rows these estimated statistical standard errors are undoubtedly smaller than the systematic errors due to real time-variations of the sea-level cosmic radiation. For the remaining rows, referring to decay electrons and disintegration neutrons, the second line of each entry gives the actual number of counts followed by the expected number of accidentals. For example, in Table I, for $(AB{:}C_{d_2})$, with Pb, focusing μ^+, there are 39 recorded coincidences and 6.4 expected accidentals. The rate, given in the first line of the entry, is $32.6 \pm(39)^{\frac{1}{2}}$, divided by 68.00.

For brevity, details of the corrections are omitted from Table II. The footnotes to Table I should suffice to illustrate the nature and order of magnitude of the corrections.

4. ANALYSIS OF THE FUNCTIONING OF THE APPARATUS

In the remainder of this paper, we consider the physical interpretation of the tabulated rates. We are

TABLE I. Measured counting rates of the first run (July 4–24, 1950).

Type of event	No absorber		Pb absorber (86 g cm^{-2})	
	focusing μ^- (68.50 hr)	focusing μ^+ (53.50 hr)	focusing μ^- (79.00 hr)	focusing μ^+ (68.00 hr)
(AB),[a] min^{-1}	31.30±0.087	33.16±0.102	31.43±0.082	34.21±0.092
$(AB:C_p)$,[b] min^{-1}	30.11±0.086	32.05±0.100	28.41±0.077	30.67±0.087
$(AB-C)$,[c] min^{-1}	1.20±0.017	1.11±0.019	3.03±0.025	3.54±0.029
(C),[d] min^{-1}	9678±7.8	9688±8.6	7591±6.9	7532±8.3
(N), min^{-1}	47.88±0.108	46.71±0.120	67.61±0.120	67.44±0.129
$(AB:C_{d1})$, hr^{-1}	0.12±0.05	0.82±0.13	0.17±0.06	2.69±0.20
(1.0–4.6 μsec)	(11–2.9)	(46–2.1)	(20–6.4)	(189–6.4)
$(AB:C_{d2})$, hr^{-1}	0	0.15±0.06	0.01±0.03	0.48±0.09
(4.5–8.0 μsec)	(1–2.9)	(10–2.1)	(7–6.5)	(39–6.4)
$(AB:N)$, hr^{-1}	1.56±0.16	1.45±0.18	6.64±0.30	4.23±0.26
(2.7–190.6 μsec)	(126–19.3)	(93–15.6)	(556–31.6)	(317–29.5)
$(ABC_p:N)$, hr^{-1}	1.48±0.16	1.31±0.17	3.56±0.22	3.42±0.24
(2.7–189.6 μsec)	(120–18.4)	(85–15.0)	(311–29.4)	(259–26.3)
$(AB-C:N)$,[e] hr^{-1}	0.08±0.04	0.14±0.05	3.06±0.20	0.81±0.11
(2.7–190.6 μsec)	(6–0.76)	(8–0.54)	(245–3.1)	(58–3.1)
$(ABC_d:N)$, hr^{-1} (delay of (C)+1.1 to delay of (C)+149.0 μsec)	0 (0–1.4×10^{-3})	0 (0–6.5×10^{-3})	0.01±0.01 (1–4.5×10^{-3})	0 (0–3.8×10^{-2})

[a] The correction for accidentals is −0.0531 min^{-1}.
[b] The correction for accidentals is −0.0072 min^{-1} for μ^- sans Pb, −0.0076 min^{-1} for μ^+ sans Pb, −0.0059 min^{-1} for μ^- with Pb, and −0.0064 min^{-1} for μ^+ with Pb. In calculating it, allowance has been made for the dead-time of the C input circuit, which prevents an accidental $(AB:C_p)$ from being detected if the (C) count follows a real $(AB:C_p)$ event. When μ^+ are focused, there is an additional correction for decay electron coincidences that appear in the prompt channel. It amounts to −0.0118 min^{-1} sans Pb and −0.0386 min^{-1} with Pb. Both corrections are included in the rates given in the table.
[c] Obtained by subtracting the corrected $(AB:C_p)$ rate from the corrected (AB) rate. Any discrepancies of 1 in the last place result from rounding-off in the table. The statistical uncertainty corresponds to the actual number of (AB) events unaccompanied by $(AB:C_p)$ events, e.g., for μ^-, sans Pb, 128,864 −123,760 =5104 and $(5104)^{\frac{1}{2}}/4110 = 0.0174$.
[d] Determined from brief tests made at intervals during the run.
[e] Obtained by subtracting the number of $(ABC_p:N)$ counts from the number of $(AB:N)$ counts.

concerned primarily with the average yield of evaporation neutrons per μ-meson captured, in its dependence on the properties of the capturing nucleus. To arrive at quantitative conclusions, we shall have to first examine in some detail the performance of the magnetic lens (Sec. 4A), the meson stopping rates (Sec. 4B), and the neutron detecting efficiency (Sec. 4C).

A. The Magnetic Lens and the Delayed Coincidence Rates

The lens was designed simply on the basis of the range-momentum relation[13] for μ-mesons, neglecting scattering. A tracing of the meson orbit in magnetized iron (Fig. 3) was laid over a drawing of the apparatus

TABLE II. Measured counting rates of the second run (August 31–October 3, 1950).[a]

Type of event	No absorber		Pb absorber (86 g cm^{-2})		Mg absorber (13.3 g cm^{-2})		Ca absorber (10.5 g cm^{-2})	
	focusing μ^- (123.42 hr)	focusing μ^+ (51.58 hr)	focusing μ^- (51.33 hr)	focusing μ^+ (46.50 hr)	focusing μ^- (182.75 hr)	focusing μ^+ (80.42 hr)	focusing μ^- (109.82 hr)	focusing μ^+ (51.75 hr)
(AB) min^{-1}	31.10±0.091	33.84±0.105	31.33±0.101	34.11±0.111	31.72±0.043	34.56±0.094	30.93±0.074	33.85±0.104
$(AB:C_p)$ min^{-1}	31.18[b]±0.090	32.95±0.103	28.62±0.096	31.06±0.105	30.32[c]±0.042	33.04[d]±0.092	29.68±0.073	32.55±0.102
$(AB-C)$ min^{-1}	0.92[b]±0.016	0.90±0.017	2.71±0.030	3.05±0.033	1.40[c]±0.014	1.51[d]±0.020	1.24±0.015	1.31±0.020
(C)[e] min^{-1}	10.08×10^3±4.9	9.72×10^3±12.7	7.55×10^3±13.7	7.57×10^3±14.7	8.91×10^3±6.5	9.33×10^3±6.2	9.68×10^3±9.8	9.70×10^3±10.7
(N) min^{-1}	46.55[f]±0.088	44.60±0.120	66.11±0.146	64.66±0.152	46.61[c]±0.082	47.67[d]±0.110	43.81±0.082	44.60±0.120
$(AB:C_{d1})$ hr^{-1}	0.02[b]±0.02	0.39[g]±0.12	0±0.02	1.16±0.16	0.44[c]±0.06	1.02[d]±0.13	0.12[h]±0.04	0.82±0.13
(1.08–1.95 μsec)	(2–0.528)	(12–0.234)	(1–0.926)	(55–0.935)	(52–1.28)	(67–0.803)	(10–0.813)	(43–0.574)
$(AB:C_{d2})$ hr^{-1}	0.04[b]±0.03	0.33[g]±0.11	0.02±0.03	0.65±0.12	0.16[c]±0.04	0.60[d]±0.10	0.041[h]±0.03	0.61±0.11
(1.91–2.81 μsec)	(3–0.547)	(10–0.242)	(2–0.957)	(31–0.966)	(20–1.32)	(40–0.831)	(4–0.841)	(32–0.594)
$(AB:C_{d3})$ hr^{-1}	0.04[b]±0.03	0.26[g]±0.09	0±0.02	0.41±0.10	0.10[c]±0.03	0.49[d]±0.09	0[h]±0.01	0.45±0.09
(2.69–3.67 μsec)	(3–0.595)	(8–0.264)	(1–1.04)	(20–1.05)	(13–1.44)	(33–0.904)	(1–0.915)	(24–0.647)
$(AB:N)$ hr^{-1}	2.09±0.15	1.86±0.22	8.65±0.43	5.06±0.36	2.37±0.13	1.99±0.18	2.46±0.16	1.91±0.21
(2.5–388.8 μsec)	(327–69.1)	(126–30.1)	(485–41.1)	(275–39.7)	(537–105)	(211–51.3)	(328–57.6)	(129–30.2)
$(ABC:N)$ hr^{-1}	1.91±0.14	1.84±0.22	4.45±0.32	4.36±0.33	1.96±0.12	1.83±0.17	2.13±0.15	1.83±0.21
(2.5–388.8 μsec)	(303–67.0)	(124–29.3)	(266–37.5)	(239–36.1)	(458–99.9)	(196–49.0)	(289–55.2)	(124–29.1)
$(AB-C:N)$ hr^{-1}	0.18±0.04	0.02±0.03	4.20±0.28	0.70±0.13	0.41±0.05	0.16±0.05	0.33±0.06	0.07±0.04
(2.5–388.8 μsec)	(24–2.14)	(2–0.822)	(29–3.61)	(36–3.54)	(79–4.65)	(15–2.25)	(39–2.38)	(5–1.17)

[a] For brevity, details of the corrections for accidentals and decay electrons, as were given with Table I, are omitted.
[b] Determined from only 62.58 hr of data.
[c] Determined from only 116.33 hr of data.
[d] Determined from only 65.08 hr of data.
[e] Determined from brief tests made at intervals during the run.
[f] Determined from only 101.25 hr of data.
[g] Determined from only 29.92 hr of data.
[h] Determined from only 75.48 hr of data.

[13] G. C. Wick, Nuovo cimento **1**, 302 (1943), as plotted by the MIT Cosmic-Ray Group. In these curves allowance is made for the density effect.

(transverse section), and by trial and error a depth for trays B was found such that no wrong-sign mesons emerging from the lens with momentum less than 219 Mev/c could pass through both A_i and B_i. As is evident from the next to last column of Table III, this momentum is barely larger than that needed to penetrate vertically the 5.7 g cm^{-2} paraffin plus the 86 g cm^{-2} Pb absorber, but is well in excess of the greatest momenta involved in stoppings in the Mg or Ca absorbers. For the measurements with our thickness of Pb it would have been wiser to make the calculations with a somewhat higher maximum momentum, but as the experimental results to be described in this section show that the focusing is essentially perfect for mesons stopping in the bottom centimeter of the Pb, we must conclude that the choice of depth for the B counters was made sufficiently conservative to allow for obliquity and scattering in the Pb.

The meson orbits considered are transverse to the magnetic field. For an inclined initial direction, the curve of Fig. 3 represents, however, the projection of the actual orbit, the momentum marked on the curve being its component in the transverse plane. This statement presupposes constancy of the rate of momentum loss along the path, a good approximation down to a total momentum of about 150 Mev/c. In addition, the concentration of mesons near the vertical ($\cos^2$ law) and the rapid falling off of telescope cross section with inclination reduce the contribution of very oblique particles.

The trajectories in magnetized iron were also computed for a rest-mass of 160 Mev/c^2 and 935 Mev/c^2, assuming again energy loss only by nonradiative atomic collisions. These were then used for a graphical study of the focusing. For 160 Mev/c^2, the focusing is almost perfect, indicating that π-mesons (mass 141 Mev/c^2) would be focused if they did not interact strongly with Fe nuclei. For 935 Mev/c^2 (protons), there is practically no focusing, because of the high momentum needed to penetrate the iron.

Multiple Coulomb scattering in the iron perturbs the orbit from the calculated "magnetic" curve. While the paraffin barrier eliminates those mesons for which the scattering effect is greatest, we nevertheless felt it necessary to make an experimental test of the focusing.

TABLE III. Ranges and momenta of the mesons stopped in the absorbers.

	Maximum vertical range beneath the paraffin		Corresponding momentum[a] on emergence from the lens	Corresponding momentum[a] on entry into the lens (approximate)
	g cm^{-2}	g cm^{-2} air equivalent	(Mev/c)	(Mev/c)
No absorber	0	0	84	492
Pb absorber	86	49	215	585
Mg absorber	13.3	12.5	130	518
Ca absorber	10.5	9.45	120	511

[a] See reference 13.

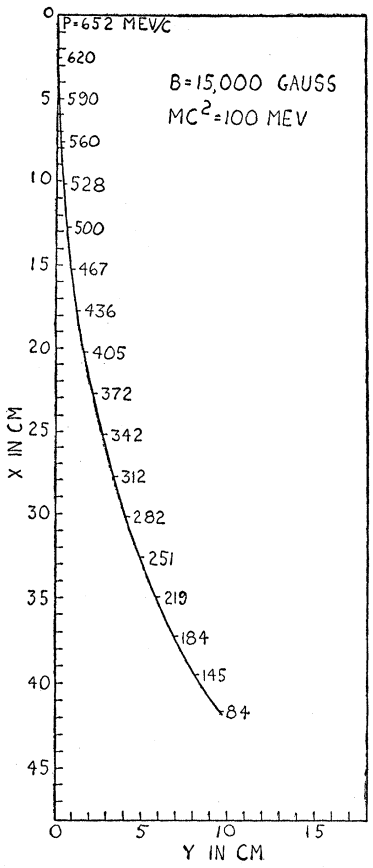

FIG. 3. Trajectory of a singly charged particle of mass 100 Mev/c^2 in iron uniformly magnetized to 15,000 gauss. The plane of the orbit is perpendicular to the magnetic field. The momentum of the particle is marked alongside the curve. As the particle progresses, its momentum decreases and along with it the radius of curvature.

For this test, we made use of the fact that in materials of high Z essentially no stopped negative μ-mesons disintegrate after 1 μsec.[14] Thus, if we detect disintegration electrons while negative mesons are being focused on Pb, we must conclude that some positive mesons are also being stopped. Since the range of the decay electrons rarely exceeds 1 cm Pb, this test only refers to the upper end of the 84–215 Mev/c band of emergent momentum. A similar test in the absence of the Pb, where only stoppings in the brass counter walls and the iron supports (1.8 g cm^{-2} air equivalent altogether) are involved, applies to the lower end of the band. The data with Ca absorber can also be used, covering a somewhat larger part of the bottom of the momentum band.

The delayed coincidence rates are given in Tables I and II and are plotted in Figs. 4 and 5. Their sums are given in Table IV. It is seen that when positive mesons are focused (the situation referred to as "μ^+"), the differential time distribution fits the mean life of 2.15 μsec, for stoppings in Pb, Fe, and brass ("no absorber"), Ca, and Mg. The absolute values of the delayed coincidence rates check reasonably well with crude estimates based on the assumption of an effective

[14] Conversi, Pancini, and Piccioni, Nuovo cimento **3**, No. 6 (1946); references to subsequent work are given in C. F. Powell, Reports on Progress in Physics **13**, 350 (1950).

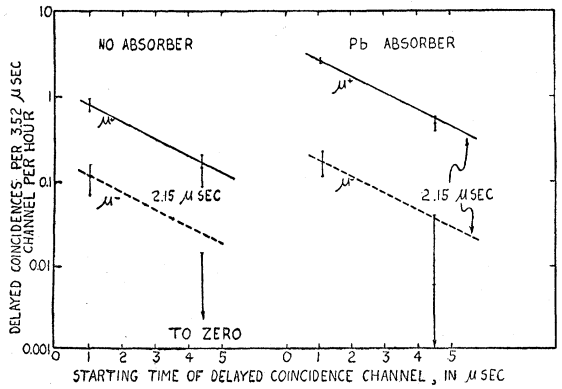

FIG. 4. Delayed coincidence data of the first run. The rate of delayed coincidences per 3.52-μsec channel width is plotted on a logarithmic scale against the starting time of the channel, to give the differential decay curve of stopped μ-mesons. As the channels do not overlap significantly, the points are statistically independent. All rates are corrected for accidental coincidences. The upper points are for the lenses focusing μ^+ mesons; the lower points for μ^-. On the left side are the rates obtained in the absence of absorber. In this case the mesons are stopped in the iron supports and the brass G-M tube walls (equivalent together to about 1.8 g cm^{-2} air). On the right side are the rates obtained when the 86 g cm^{-2} Pb absorber is inserted. Straight lines of slope corresponding to the natural mean life of 2.15 μsec are drawn in.

range for the decay electrons of 10 g cm^{-2} Pb and 12 g cm^{-2} Mg or Ca. When negative mesons are focused ("μ^-"), the delayed coincidence rates are so low, except in the case of Mg, that it is difficult to draw conclusions about the shape of the time distribution. The data of the first run (Fig. 4) do suggest that counter lags contribute appreciably to the μ^- delayed coincidence rate. The data of the second run (Fig. 5) for Ca give the same impression; they are decidedly incompatible, both in magnitude and slope, with the 0.2 or 0.3 μsec mean life of negative μ-mesons in calcium.[14] For Mg (Fig. 5), the observed μ^- rates fit the reported 1.0 $\pm$0.1 μsec mean life[14,15] very well; and the ratio of the μ^- to μ^+ delayed coincidence rates, 0.33$\pm$0.05, is in excellent agreement with the value 0.28$\pm$0.06 expected on the assumption of competition between capture and decay, with $\tau_-=1.0\pm0.1$ μsec, $\tau_0=2.15\pm0.07$ μsec, and a positive:negative stopping ratio of 1.23.

An upper limit for the leakage factor, the fraction of wrong-sign mesons that stop, relative to the number of them stopping when they are right-sign, is found by ignoring the contribution of counter lags to the μ^- delayed coincidence rate. It is the ratio of the μ^- delayed coincidence rate to the μ^+ delayed coincidence rate, shown in the last column of Table IV. With the Pb absorber in place, this upper limit is $5.6^{+2.7}_{-2.3}$ percent for the first run, but is decreased to $0.9^{+2.1}_{-0.9}$ percent in the second run, a result, no doubt, of the reduction in lags associated with the increase in sensitivity of the C preamplifier. It appears, then, that the leakage is essentially zero for mesons stopping in the bottom centimeter or so of lead. With no absorber, the upper limit appears to be higher. One would expect the disturbing effect of Coulomb scattering to show itself here if at all, though the observed effect could be entirely statistical. The weighted mean of the upper limits for the Ca and no absorber data of the second run is $(8.8^{+3.3}_{-2.8})$ percent; it applies to the mesons stopped in the top centimeter or so of lead. Since the range distribution of the slow mesons emerging from the lens is essentially flat, the effective upper limit on the leakage factor, as regards stoppings in the whole Pb absorber, is about 5 percent. As regards neutron production by stopped mesons, more weight must be given to the bottom of the Pb, as the efficiency for detecting neutrons decreases with increasing height of the neutron source in the absorber. The measurements with a Ra-α-Be source (described below) show that the efficiencies are in the proportion 2.3:1.7:1 for the bottom, middle, and top of the Pb absorber. Thus, as regards $(AB-C:N)$ events in Pb, the effective leakage factor is less than about 2 percent. For Mg and Ca, the corresponding figure is about 9 percent.

Independent evidence on the quality of the focusing is provided by the very effect with which the present experiment is concerned. The $(AB-C:N)$ rate refers to nuclear disintegrations produced by stopped particles, which are, under the conditions of this experiment, preponderantly μ-mesons. Since positive μ-mesons do not produce nuclear disintegrations, the μ^+ $(AB-C:N)$ rate must be due to leakage μ^- mesons and to other types of particles. Hence an upper limit on the leakage factor is given by the ratio of the μ^+ $(AB-C:N)$ rate to the μ^- one. The rates in question are presented in Tables I and II. The lowest value of the $\mu^+:\mu^-$ ratio is that obtained with Pb in the second run, (16.6$\pm$3.3)

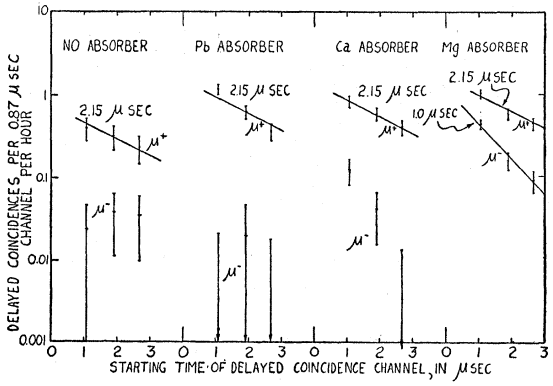

FIG. 5. Delayed coincidence data of the second run. The rate of delayed coincidences per 0.87 μsec channel width is plotted on a logarithmic scale against the starting time of the channel, to give the differential decay curves of stopped μ-mesons. As the channels do not overlap significantly, the points are statistically independent. All rates are corrected for casuals. The upper points are for the lenses focusing μ^+ mesons; the lower points for μ^-. Four sets of data are plotted: from left to right, no absorber (1.8 g cm^{-2} air equivalent Fe and brass), Pb absorber (86 g cm^{-2}), Ca absorber (10.5 g cm^{-2}), and Mg absorber (13.3 g cm^{-2}). Straight lines of slope corresponding to a mean life of 2.15 μsec are fitted to the μ^+ rates. For μ^-, Mg absorber, a line corresponding to a mean life of 1.0 μsec is fitted.

[15] A. H. Benade and R. D. Sard, Phys. Rev. 76, 489 (1949).

percent. The fact that this upper limit on the leakage factor is well above that given by the delayed coincidence data proves that an appreciable part of the (relatively small) μ^+ $(AB-C:N)$ rate with Pb is not due to stopped mesons.

In comparing the anticoincidence rates with the spectral intensity of mesons at sea level, we shall need to know how the aperture of the lens varies with incident momentum. For right-sign particles, the aperture decreases smoothly toward the limiting value corresponding to no curvature in the iron. For wrong-sign particles the aperture is zero up to a certain momentum, and then increases smoothly toward the same limiting value. In order to calculate these two curves, we have extended the μ-meson trajectory of Fig. 3 back to 2000 Mev/c, and have used it, on a 1:1 scale drawing of the lens, to determine the angular opening in the transverse section as a function of incident momentum. The results are shown in Fig. 6. When these values are weighted in accordance with the momentum spectrum,[16] we find for the effective lens aperture of μ-mesons that produce (AB) events, 10.8° for a right-sign mesons and 4.6° for wrong-sign mesons. Here the assumption has been made that the spectra for positive and negative mesons have the same shape (constant positive excess).[17] For the mesons that stop in the Pb absorber, the effective apertures are 26.2° (right-sign) and 0° (wrong-sign). For Mg and Ca, the opening is slightly larger for right-sign stopped mesons, about 27.0°.

TABLE IV. Data bearing on the leakage factor of the lens.

	Delayed coincidence rate, hr^{-1} (1.0 −8.0 μsec in first run, 1.07 −3.67 μsec in second run)	$\mu^-:\mu^+$ ratio of the delayed coincidence rates, %
First run:		
No absorber, μ^-	0.09±0.05	+7.7
		9.3
No absorber, μ^+	0.97±0.14	−5.7
Pb absorber, μ^-	0.18±0.07	+2.7
		5.6
Pb absorber, μ^+	3.16±0.22	−2.3
Second run:		
No absorber, μ^-	0.10±0.05	+8.1
		10.3
No absorber, μ^+	0.98±0.18	−5.5
Pb absorber, μ^-	0.02±0.04	+2.1
		0.9
Pb absorber, μ^+	2.22±0.22	−0.9
Ca absorber, μ^-	0.16±0.05	+4.1
		8.8
Ca absorber, μ^+	1.88±0.19	−3.3
Mg absorber, μ^-	0.70±0.08	
Mg absorber, μ^+	2.11±0.18	33±5

[16] J. G. Wilson, Nature **158**, 414 (1946).
[17] J. G. Wilson, Proc. Phys. Soc. (London) **64A**, 417 (1951).

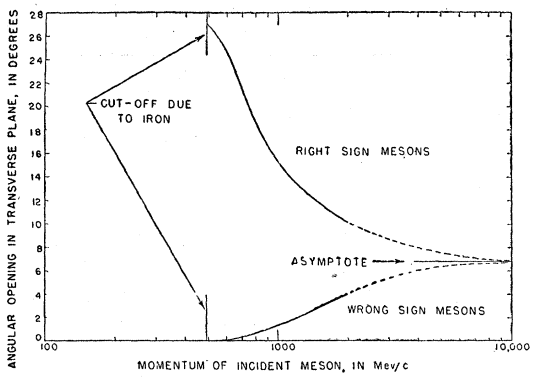

FIG. 6. Aperture of the lens as a function of the momentum of the incident μ-meson. The upper curve refers to "right-sign" mesons, i.e., those of the polarity being focused, the lower one to "wrong-sign" mesons. The curves start at the minimum momentum needed to penetrate the iron and the paraffin barrier. Beyond 2000 Mev/c they are simply an artistic extrapolation. The common asymptote corresponds to zero deviation in the iron.

B. The Meson Stopping Rates

For determining relative values for different elements of the mean number of evaporation neutrons per μ-meson captured, we need only assume that the mean stopping rate is proportional to the corrected anticoincidence rate, $\Delta(AB-C)=(AB-C)$ with absorber minus $(AB-C)$ sans absorber. Strong support for this assumption is provided by the fact that the corrected anticoincidence rates for both μ^- and μ^+ (Table VIB, second column) are indeed in the ratio of the equivalent absorber thicknesses (Table III, third column). The ratios are shown in Table V.

One can go further, and seek to determine the absolute value of the mean neutron multiplicity. This requires knowledge of the actual meson stopping rate, as well as of the absolute neutron detecting efficiency. The former can be determined by comparison of our corrected anticoincidence rates with the known sea-level meson spectrum.[16,18,19] This comparison involves two steps—determination of the total meson flux, and determination of the fraction of it expected to stop in the absorber.

We first calculate the expected (AB) rate in the absence of magnetic field. As all the particles, whether they subsequently stop or not, must penetrate at least 239 g cm^{-2} Fe, we may assume[19] a cosine-squared zenith angle dependence for I_v, the intensity per unit transverse area per unit solid angle. And as the widths of the counter trays A_i and B_i are small compared to their vertical separation, we may replace them by flat rectangular sensitive areas and assume the intensity and projected area to vary linearly across any transverse slice. When there is no magnetic field, a straightforward double integration along the lines indicated by Greisen[20] gives

$$(A_iB_i)=I_v\frac{bd}{4}[3\varphi\tan\varphi-\cos^2\varphi]_{\varphi=\arctan[(a+c)/2l]}^{\varphi=\arctan[(a-c)/2l]}$$
$$=31.1I_v,$$

[18] B. Rossi, Revs. Modern Phys. **20**, 537 (1948).
[19] W. L. Kraushaar, Phys. Rev. **76**, 1045 (1949).
[20] K. Greisen, Phys. Rev. **61**, 212 (1942).

TABLE V. Comparison of the different absorbers as regards stopping rates.

	Mg:Pb	Ca:Pb
Ratio of air-equivalent absorber thicknesses, corrected for Coulomb scattering	0.24	0.18
Ratio of the corrected anticoincidence rates, μ^-, second run	0.27±0.01	0.18±0.01
Ratio of the corrected anticoincidence rates, μ^+, second run	0.29±0.01	0.19±0.01

where a=sensitive length of top tray=101.6 cm; b=sensitive width of top tray=4.92 cm; c=sensitive length of bottom tray =50.8 cm; d=sensitive width of bottom tray=4.92 cm; and l=vertical distance between counter axes=43.2 cm. This expression reduces to Greisen's when $c=a$, $d=b$. The dimensionless factor in brackets involves only the lengths of the trays and their vertical separation. The transverse dimensions enter only in the factor bd. A measurement of (AB) without magnetic field gave 29.2 min^{-1}, while the value $I_v=7.7\times10^{-3}$ cm^{-2} sec^{-1} sterad^{-1} read from Rossi's curve[18] at a range of 192 g cm^{-2} air[21] leads to (AB) =28.8 min^{-1}. The extreme closeness of the agreement (to within 1.5 percent) must be regarded as fortuitous, as the measurement did not last long enough for meteorological variations to average out. These figures are entered in the first row of Table VIA.

When the magnetic field is on, the geometrical situation is more complicated, the allowed cone for each momentum and each point of the A_i counter tray being in general multiply connected. But none of the allowed directions in the transverse plane is strongly inclined from the vertical, and it is, therefore, a good approximation simply to use the above formula with b replaced by l times the tangent of the effective net aperture in the transverse plane. Thus, for right-sign particles, $b_{eff}=43.2\times\tan10.8°$ =8.2 cm, while for wrong-sign particles, $b_{eff}=43.2\times\tan4.6°=3.5$ cm. Assuming[17] a positive:negative ratio of 1.23 constant over the incident momentum spectrum, we then compute, for "μ^+," $(AB)=77I_v$, for "μ^-," $(AB)=71I_v$. In the second and third rows of Table VIA the (AB) rates averaged over both runs are compared with those predicted by these expressions with $I_v=7.7\times10^{-3}$ cm^{-2} sec^{-1} sterad^{-1}. There is seen to be agreement to within 5 percent. Furthermore, the ratio of the observed μ^+ to the observed μ^- (AB) agrees perfectly with that predicted by our calculation.

When we consider now the fraction expected to stop, difficulties arise. At the range in question the best determinations of the absolute differential range spectrum are spread over a whole power of 2 (see, e.g., the points plotted in Fig. 6 of reference 18). The elegant G-M tube experiments of Kraushaar[19] do, however, give strong support to the value adopted by Rossi and Sands (curve of Fig. 6 of reference 18). A slightly lower value results from combining the momentum spectrum determined by the cloud chamber technique[16] with the range-momentum relation.[13] We shall compare our apparent stopping rates with both the Rossi-Sands-Kraushaar counter value and the Wick-J. G. Wilson cloud-chamber value for the meson stopping rate. In both cases allowance will be made for the increase in path length in the absorber resulting from Coulomb scattering (10.3 percent in Pb 2 percent in Ca, 1.4 percent in Mg). In the comparison with our rates, an additional uncertainty is introduced by the fact that the lens aperture for right-sign stopped mesons is so large that the approximation we have used, $b_{eff}=l\tan\alpha$, where α is the net aperture in the transverse section, becomes only fair. Some improvement is to be expected from use of the following expression, obtained by integrating the cosine squared distribution across a transverse section:

$$b_{eff}=l\tan\alpha\left[1-\frac{2}{5}\left(1-\frac{\sin\alpha}{\alpha}\right)-\frac{3}{10}\left(1-\frac{\sin2\alpha}{2\alpha}\right)\right].$$

The following sample calculation will illustrate the procedure used in computing the expected values of Table VIB. Consider the case μ^-, Pb. The fraction of the (AB) rate due to negative mesons is 0.66 (this figure follows from a 1.23 positive:negative ratio and the effective apertures 10.8° and 4.6° for right-sign and wrong-sign mesons). These are in an aperture of 10.8°, while the stopped negative mesons are in an aperture of 26.2°. The ratio of the b_{eff} for these two values of α is 2.46, so that the fraction of (AB) that stops is equal to the absorption coefficient for the ranges in question multiplied by $2.46\times0.66=1.62$. The counter value for the absorption coefficient is 3.96 percent (from $i_v=5.7\times10^{-6}$ (g air)$^{-1}$ sec^{-1} sterad^{-1}, $I_v=7.7\times10^{-3}$ cm^{-2} sec^{-1} sterad^{-1}, effective thickness=53.3 g cm^{-2} air), while the cloud-chamber value is 3.38 percent (corresponding to a momentum band from 492 to 595 Mev/c) with a purely statistical error of about 6 percent. Thus the expected meson stopping rate for the second μ^-, Pb run is $31.33\ \text{min}^{-1}\times1.62\times3.96\times10^{-2}=2.01\ \text{min}^{-1}$ (counter value) or $31.33\ \text{min}^{-1}\times1.62\times3.38\times10^{-2}=1.72\ \text{min}^{-1}$ (cloud-chamber value).

It is seen from the results collected in Table VIB that the observed anticoincidence rates are nicely bracketed by those expected on the basis of the two assumed absorption coefficients, which differ by 16 percent. This agreement, like that in Table VIA, does not involve the use of any adjustable parameter. We conclude that the constant of proportionality relating our apparent stopping rate, $\Delta(AB-C)$, to the actual meson stopping rate is equal to unity to within about 20 percent, perhaps more closely. The loss due to failure of the C tray to intercept all scattered mesons[19] appears to be compensated by the gain due to side showers and knock-on electrons.

Between the first and second run the gain of the C tray amplifier was increased, with the result that the anticoincidence efficiency improved, and the $(AB-C)$ rates decreased (compare Tables I and II). For μ^-, the apparent stopping rate, $\Delta(AB-C)$ is essentially unchanged, 1.79±0.034 min^{-1} as against 1.83±0.031 min^{-1}. For μ^+ there is a discrepancy, the new $\Delta(AB-C)$ being 2.15 ±0.037 min^{-1} as compared with 2.42±0.035 min^{-1} for the old. We know of no objective reason for rejecting any of the data, and are forced to conclude that some unnoticed defect, perhaps in the $(AB:C_p)$ scaler, occurred during one of the two μ^+, Pb runs. The positive:negative ratios, shown in the last column of Table VIB lend some support to the view that the data of the second run are to be preferred, as the ratio 1.32±0.03 is out of line with other determinations.[17] As our main concern is with stopped negative mesons, we do not need to occupy ourselves further with this point.

The positive:negative ratios of the second run (Table VIB) are in excellent agreement with each other and with other observations.[17]

C. The Neutron Detecting Efficiency

As the evaporation neutrons to which our apparatus responds are expected to have energies in the neighborhood of 1–2 Mev, and as our detecting efficiency should be fairly constant up to about 5 Mev, use of a Ra-α-Be source for an efficiency determination seems justified. We used one of 70 μc strength, emitting 1.69×10^3

[21] The average path length through the Fe is 1.09×the vertical thickness, corresponding to 209 g cm^{-2} air. The site is, however, 21−4=17 g cm^{-2} air above sea-level.

neutrons/sec.[22] It was placed at various positions in the absorber, and the efficiency determined for each. We found only a slight dependence on position in the horizontal plane, but a strong dependence on depth in the absorber.[12] With Pb, the efficiencies for the source at the bottom, middle, and top of the absorber are in the ratio 2.3:1.7:1; with Mg, the corresponding figures are 1.8:1.5:1; with Ca, the bottom: top ratio is 1.6:1. Some, but not all, of the effect can be ascribed to solid angle changes. As the range distribution of slow mesons incident on the absorber is essentially flat, the efficiencies for different depths can simply be averaged. We find, then, an effective efficiency of 2.20 percent, *the same, within 1 percent, for all three absorbers.*

In the comparison of the multiplicities from the different absorbers, any systematic errors in the efficiency determination, whether connected with the absolute strength of the test source or the spectrum of evaporation neutrons, cancel out in the first order.

When the neutrons are counted in a gate of finite duration, as is the case for the neutron coincidences, the efficiency is reduced, because of the loss of counts from neutrons captured after the gate has ended. The factor of reduction is $1-\exp(-T/\tau)$, where T is the gate length and τ the neutron mean life. The latter has been determined by comparing the $(AB:N)$ rates, with Pb, of the first and second runs, T being 187.9 and 386.3 μsec, respectively. The result is $\tau=152^{+37}_{-35}$ μsec, in agreement with the values found by other investigators with similar detectors.[23,24] A third set of data, with $T=1042$ μsec, was also taken, and it was verified that the $(AB:N)$ rate at this third value of T fitted very well on the curve of form $1-\exp(-T/152)$ drawn through the first and second points. The coherent efficiency is therefore reduced by the factor $(0.71^{+0.09}_{-0.08})$ for the first run and $(0.92^{+0.04}_{-0.05})$ for the second, giving the efficiency values $(1.56^{+0.20}_{-0.17})$ percent and $(2.03^{+0.09}_{-0.11})$ percent for the first and second runs, respectively.

5. NEUTRON PRODUCTION IN MESON CAPTURE

The neutron production by particles stopped in the absorber is given by the increase in the $(AB-C:N)$ rate when the absorber is inserted. That part of the effect due to stopped negative μ-mesons is the increase in this difference in switching from μ^+ to μ^-. The $(AB-C:N)$ rates (from Tables I and II), the rates resulting from the absorber, and the rates resulting from negative mesons stopped in the absorber are shown in Table VII.

A. Meson Capture in Lead

In both runs the rates with Pb are much larger than the background rates sans Pb, and there is a striking increase in the Pb effect in going from μ^+ to μ^-. This increase constitutes a confirmation[25] of the interpretation of earlier experiments[1] on neutron production by charged cosmic-ray particles as showing neutron production resulting from μ-meson capture.

While the present experiment was not designed primarily for an absolute determination of the mean number of neutrons per capture, the results of the analyses of Sec. 4 show that it is possible to calculate this quantity from our data with fair accuracy. The assumptions made in the calculation are: (a) the μ^- anticoincidence difference ($\Delta(AB-C)$) equals the rate of stopping of negative μ-mesons; (b) the increase in $\Delta(AB-C:N)$ in going from μ^+ to μ^- is the rate of neutron production by stopped negative μ-mesons; (c) the neutron detecting efficiency is sensibly the same for the meson-capture neutrons as for Ra-α-Be neutrons. On the basis of the analyses of the previous paragraphs, we conclude that the systematic error resulting from these assumptions is probably not greater than 25 percent. Thus,

TABLE VI. Comparison of telescope rates with those expected for μ-mesons.

	A. (AB) rate	
	Observed min^{-1}	Expected[a] min^{-1}
$B=0$	29.2	28.8
μ^+	34.0	35.7
μ^-	31.3	32.8

	B. $\Delta(AB-C)$ rate			
	Observed min^{-1}	Expected[b] min^{-1}	Expected[c] min^{-1}	Observed positive:negative ratio
First run:				
Pb, μ^-	1.83±0.031	2.02	1.72	1.32±0.029
Pb, μ^+	2.42±0.035	2.49	2.12	
Second run:				
Pb, μ^-	1.79±0.034	2.01	1.72	1.20±0.031
Pb, μ^+	2.15±0.037	2.48	2.11	
Ca, μ^-	0.32±0.022	0.37	0.31	1.29±0.080
Ca, μ^+	0.41±0.027	0.46	0.39	
Mg, μ^-	0.48±0.021	0.50	0.43	1.28±0.121
Mg, μ^+	0.62±0.026	0.61	0.52	

[a] Assuming $I_0=7.7\times10^{-3}$ cm^{-2} sec^{-1} sterad^{-1}, as read from Fig. 5 of reference 18 at $R=192$ g cm^{-2} air.

[b] Assuming an absorption coefficient of 7.4×10^{-4} cm^2 (g air)$^{-1}$, as read from Rossi's curves (Figs. 5 and 6 of reference 18). The vertical thickness of absorber is increased to allow for Coulomb scattering (10.3 percent in Pb, 2 percent in Ca, 1.4 percent in Mg) and is then translated to its air equivalent.

[c] Assuming, on the basis of J. G. Wilson's momentum spectrum (see reference 16), that the ratio of the number of mesons in a 100 Mev/c band centered at 540 Mev/c to the number above 490 Mev/c is 47/1426. The momentum band involved in stoppings in the Pb is taken to be 492–595 Mev/c. The fraction stopping in Ca and Mg is then obtained from that for Pb by applying the ratio of air-equivalent thicknesses after allowance has been made for scattering.

[22] This calibration refers ultimately to the Argonne National Laboratory's "Source No. 38," whose strength is known to only about 10 percent.

[23] M. F. Crouch, Phys. Rev. **81**, 134 (1951); M. F. Crouch and R. D. Sard, Phys. Rev. **85**, 120 (1952).

[24] Cocconi, Tongiorgi, and Widgoff, Phys. Rev. **79**, 768 (1950).

[25] The cloud-chamber pictures of E. J. Althaus (thesis, Washington University, September, 1950) and the underground counter measurements of M. F. Crouch (references 12 and 24) also confirm the production of disintegration neutrons in μ-meson capture in lead. In the meanwhile, Groetzinger, Berger, and McClure (see reference 26) have obtained statistically significant data with a magnetized-iron lens, that also confirm the effect.

TABLE VII. Neutron production by stopped particles.

		Neutrons associated with anti-coincidences ($(AB-C:N)$ hr^{-1})	Neutrons associated with stoppings in the absorber ($\Delta(AB-C:N)$, hr^{-1})	Neutrons associated with negative mesons stopped in the absorber ($\Delta^2(AB-C:N)$, hr^{-1})
First run:				
Pb	μ^- with Pb	3.06±0.20	2.99±0.20	2.32±0.24
	μ^- sans Pb	0.08±0.04		
	μ^+ with Pb	0.81±0.11	0.67±0.12	
	μ^+ sans Pb	0.14±0.05		
Second run:				
Pb	μ^- with Pb	4.20±0.28	4.02±0.29	3.34±0.31
	μ^- sans Pb	0.18±0.04		
	μ^+ with Pb	0.70±0.13	0.68±0.13	
	μ^+ sans Pb	0.02±0.03		
Ca	μ^- with Ca	0.33±0.06	0.16±0.07	0.11±0.09
	μ^- sans Ca	0.18±0.04		
	μ^+ with Ca	0.07±0.04	0.05±0.05	
	μ^+ sans Ca	0.02±0.03		
Mg	μ^- with Mg	0.41±0.05	0.23±0.06	0.09±0.08
	μ^- sans Mg	0.18±0.04		
	μ^+ with Mg	0.16±0.05	0.14±0.06	
	μ^+ sans Mg	0.02±0.03		

first run:

$$\langle m\rangle_{Av}=\frac{2.32\pm0.24}{(1.83\pm0.03)\times60\times(1.56\pm0.19)\times10^{-2}}$$

$$=1.36\pm0.22.$$

Second run:

$$\langle m\rangle_{Av}=\frac{3.34\pm0.31}{(1.79\pm0.03)\times60\times(2.03\pm0.10)\times10^{-2}}$$

$$=1.53\pm0.16.$$

The errors indicated are purely statistical. In addition to the systematic errors discussed above, there is an uncertainty in the neutron standard[22] estimated at 10 percent. The results of the two runs are seen to agree; the weighted mean of the two is 1.47±0.13.

This result compares with the value 2.16±0.15 obtained by Crouch[23] in an experiment designed for an absolute determination of $\langle m\rangle_{Av}$. In the comparison of the two experiments the uncertainty in the primary neutron standard cancels out, as the same Ra-α-Be source was used in the two efficiency measurements. The other systematic errors do, however, remain, and the two results cannot be called definitely inconsistent. Crouch's geometry is superior to ours from the point of view of determining the absolute number of meson stoppings and also as regards "flatness" of neutron response, so we feel that his value is probably nearer the true one.

In this connection we note that even a small leakage of wrong-sign mesons will lower our apparent $\langle m\rangle_{Av}$. Thus, if the leakage in $\Delta(AB-C)$ is 5 percent and that in $\Delta(AB-C:N)$ is 2 percent, the apparent $\langle m\rangle_{Av}$ is decreased by 8 percent.

Both values are consistent with the 1.96±0.72 (probable error) found by Groetzinger *et al.*[26] Our value is nearer to the 0.95 predicted[23] on a crude calculation of the neutron evaporation resulting from the nuclear excitation in the reaction $\mu^-+P\rightarrow N+\nu$.

B. Meson Capture in Iron and Brass

The increase in coherent efficiency in the second run, together with better statistics, brought to light neutron production by μ-meson capture in the iron supports for the absorber or the brass G-M tube walls (1.8 g cm^{-2} air altogether). Thus the sans-absorber $(AB-C:N)$ rate goes from 0.02±0.03 hr^{-1} to 0.18±0.04 hr^{-1} when the focusing field is switched from μ^+ to μ^-. The μ^- rate is based on 24 events, with 2.14 expected accidentals.

C. Meson Capture in Magnesium

Magnesium was the first absorber of low Z to be studied. While the $(AB-C:N)$ rate shows a definite increase on switching from μ^+ to μ^-, this increase is not much larger than that in the absence of absorber. The neutron production in the iron supports and brass counter walls (1.8 g cm^{-2} air equivalent) is comparable with that in the magnesium (12.5 g cm^{-2} air equivalent). The net effect ascribable to μ-mesons in Mg is only 0.09±0.08 hr^{-1}. This must be compared with the rate at which mesons are captured, equal to the meson stopping rate times the fraction that escapes decay, $1-(\tau_-/\tau_0)$. With $\tau_-=1.0$ μsec, our data give 0.535 $\times(0.48\pm0.02)$ min$^{-1}=15.4\pm0.6$ hr^{-1}. The ratio of detected neutrons to captured mesons is, therefore, (0.6±0.5) percent. In contrast, the same ratio for Pb (second run) is (3.1±0.3) percent. Thus, the average neutron multiplicity from μ-meson capture in Mg is considerably smaller than that for Pb; in effect, the ratio of the two multiplicites is 0.2±0.2. It appears safe to conclude that the Mg multiplicity is with high probability less than one-half the Pb multiplicity. Evidently further measurements with a geometry giving a higher ratio of Mg effect to background are needed.

D. Meson Capture in Calcium

When it was found that the neutron yield from Mg is small in comparison with Pb, the suspicion arose that the difference might be due to the relatively high excitation energy needed to liberate a neutron from the capturing Mg nucleus (5.5 Mev for $_{11}Na^{24}-{}_{12}Mg^{24}$ mass difference+6.9-Mev neutron binding energy=12.4 Mev, as compared with 8.4 Mev for Pb). At Feenberg's

[26] Groetzinger, Berger, and McClure, Phys. Rev. **81**, 969 (1951).

suggestion we have, therefore, taken data with Ca, a nucleus for which the energy threshold is only 7.3 Mev. If the height of the threshold explains the effect, Ca should be a copious neutron emitter.

The results are seen to be very similar to those for Mg. The neutron production in the Ca (9.45 g cm^{-2} air equivalent) is hardly greater than that in the Fe and brass, and the net effect ascribable to μ-mesons stopped in Ca is only 0.11 ± 0.09 hr^{-1}. With $\tau_-=0.2$ μsec,[14] the fraction of stopped mesons that are captured is 0.91, so the rate of meson capture is $0.91\times(0.32\pm0.02)$ min^{-1} $=17.5\pm1.2$ hr^{-1}. The ratio of detected neutrons to captured mesons is therefore (0.6 ± 0.5) percent, exactly the same as for Mg. For Ca too, the neutron multiplicity is considerably smaller than that for Pb, and is with high probability less than one-half the Pb multiplicity.

E. Discussion

These preliminary results with Mg and Ca indicate a considerably lower neutron yield from these light α-particle nuclei than from Pb. Heidmann (private communication) has remarked that at low Z proton emission will reduce the neutron yield, and his calculation of $\langle m\rangle_{Av}$ for μ-meson capture in Ca gives, on the basis of the excitation energy distribution corresponding to $\mu^-+P\rightarrow N+\nu$ in a Fermi gas, a value somewhat above 0.5. A similar calculation for Pb by Crouch[23] gives 0.95. It is hard to understand why the statistical model should give for Pb too low a value and for Ca one that is probably too high.

Primakoff (private communication) has pointed out that for both Mg and Ca there is a large change in angular momentum between the original nucleus and the ground state of the nucleus formed by capture of the meson. Because of the large momentum and hence angular momentum of the recoiling neutrino, it is possible that transitions to the ground state or to states near the ground state are favored. This would give low average excitation and hence little neutron emission.

6. OTHER RESULTS

Referring to Tables I and II, it is seen that the $(ABC:N)$ rates—neutrons associated with one or more penetrating particles—are sensibly independent of the sense of the magnetic field. This is to be expected, as only slow mesons are focused. One notices also that there is essentially no contribution to the $(ABC:N)$ rate from the Mg or Ca absorbers.

The $(ABC_d:N)$ rates of Table I show that, as expected, there are no neutrons associated with meson decay.[27]

The incoherent (N) rates of Tables I and II are essentially the same for no absorber, Ca (10.5 g cm^{-2}), and Mg (13.3 g cm^{-2}), but are 35 percent higher when the Pb absorber is in place. Most of this increase is probably due to nuclear disintegrations in the Pb produced by cosmic-ray particles, an effect studied thoroughly by Cocconi Tongiorgi[28] with a similar geometry. The capture of μ-mesons cannot account for any appreciable part of the increase, which is probably due mainly to cosmic-ray nucleons. In order to find out how much of it is because of charged particles, the trays A were disconnected and $(B:N)$ events were recorded. The rate observed was 33 ± 1 hr^{-1}, in contrast with the increase in (N) of 1043 hr^{-1}. After allowance is made for the difference in area of the B trays and the Pb absorber and for the loss of efficiency in coherent counting, we find that about 20 percent of the neutron production in the Pb is due to charged particles, in agreement with observations on stars in emulsions.

7. CONCLUSIONS

Our main conclusions are:

1. The production of neutrons by μ-meson capture in Pb is confirmed.

2. The average number of neutrons emitted per capturing Pb nucleus is 1.47 ± 0.13, with an additional systematic error of about 10 percent in the standard of neutron flux and further systematic errors resulting from the geometry that amount to not more than 25 percent. This result is, therefore, not incompatible with the value 2.16 ± 0.15 obtained by Crouch in a measurement underground. We feel that more weight should be given to his result.

3. In both Ca and Mg there is little, if any, neutron production in μ-meson capture. The ratio of neutrons detected to mesons captured is for both absorbers (0.6 ± 0.5) percent, in contrast with the value (3.1 ± 0.3) percent for Pb. The neutron detecting efficiencies are the same in the three cases. Thus, the neutron multiplicity from capture in these α-particle nuclei is with high probability small compared to that from Pb.

8. ACKNOWLEDGMENTS

We are deeply indebted to Mr. J. D. Miller for the construction of almost all of the circuits and for his contributions to their design and maintenance. We are grateful to Mr. A. H. Benade for the construction of the iron lenses, and to Messrs. Benade and Miller for the design and construction of the current supplies. Dr. W. Keller of the Mallinckrodt Chemical Company assisted materially in the procurement of the calcium metal. Finally, we should like to thank Dr. Jean Heidmann for communicating to us before publication the results of his calculations on neutron evaporation from Ca.

[27] V. Tongiorgi-Cocconi and W. L. Kraushaar have previously obtained the same result (private communication).

[28] V. Cocconi Tongiorgi, Phys. Rev. **76**, 517 (1949).